A Fast and Flexible Computer Vision System for Implanted Visual Prostheses

Wai Ho Li(✉)

Monash Vision Group, Monash University, Melbourne, Australia
wai.ho.li@monash.edu

Abstract. Implanted visual prostheses generate visual percepts by electrically stimulating the human visual pathway using an array of electrodes. The resulting bionic vision consists of a spatial-temporal pattern of bright dots called phosphenes. This patient-specific phosphene pattern has low resolution, limited dynamic range and is spatially irregular. This paper presents a computer vision system designed to deal with these limitations, especially spatial irregularity. The system uses a new mapping called the Camera Map to decouple the flexible spatial layout of image processing from the inflexible layout of phosphenes experienced by a patient. Detailed simulations of a cortical prosthesis currently in preclinical testing were performed to create phosphene patterns for testing. The system was tested on a wearable prototype of the cortical prosthesis. Despite having limited computational resources, the system operated in real time, taking only a few milliseconds to perform image processing and visualisations of simulated prosthetic vision.

Keywords: Visual prosthesis · Bionic eye · Cortical implant · Simulated prosthetic vision · Wearable computer vision · Integral images · Irregular · Camera maps · Real time · Phosphene maps · Image processing

1 Introduction

According to the World Health Organization, visual impairment and blindness affect nearly 300 million people worldwide[1]. Some causes of vision loss, such as cataracts, can already be treated using existing medical technology. Implanted Visual Prostheses (IVP) attempt to address currently incurable diseases, such as Retinitis Pigmentosa (RP), by electrically stimulating the still-healthy parts of a patient's visual pathway to produce prosthetic vision.

Prosthetic vision has many limitations, which are further detailed in Section 2. These limitations severely restrict the *bandwidth* of visual information that can be provided to a patient. Computer Vision provides a promising way to improve the usefulness of prosthetic vision despite its limitations. This paper presents a computer vision system for implanted visual prostheses. The system can be

[1] http://www.who.int/mediacentre/factsheets/fs282/en/

L. Agapito et al. (Eds.): ECCV 2014 Workshops, Part III, LNCS 8927, pp. 686–701, 2015.
DOI: 10.1007/978-3-319-16199-0_48

flexibly tailored in a patient-specific manner and operates in real time on a computationally limited wearable prototype. The research contributions, design and testing of the system are detailed in Section 3.

Ever since 1755, when LeRoy discharged a Leyden Jar to cause a blind patient to see "flames passing rapidly downward" [15], numerous experiments have confirmed that electrical stimulation of the human visual pathway can result in visual percepts. Modern implanted visual prosthesis (IVP) operate using the same fundamental principle. Controlled electrical stimulation is applied using small implanted electrodes to produce a bright visual percept called a *phosphene*. By apply temporally varying stimuli using an array of electrodes, the patient *sees* spatial-temporal patterns of phosphenes similar to a low resolution dot display.

In the late 1960's, Brindley and Lewin [2] developed the first IVP. The system used an array of electrodes on the visual cortex to elicit multiple phosphenes at different locations of a patient's visual field. However, the IVP was only suitable for laboratory use as the stimulation electronics were not portable. The IVP also did not include a portable camera.

From the 1970's to the early 2000's, Dobelle developed several IVP devices that used implanted cortical electrode arrays, including systems that generate electrical stimuli based on imagery captured with a headworn camera [9]. Despite a range of problems including the heaviness of the portable electronics and the use of wired transcranial connections, a patient's biography suggests that the device did provide useful vision [21].

Recent research and development have focused on IVP that electrically stimulate either the retina or the visual cortex[2]. The reason for the focus on retinal and cortical stimulation is that electrical stimulation at these two anatomical locations can give reliable spatial patterns of phosphenes. Retinal prostheses, such as the Argus II device from Second Sight, have already been implanted into several tens of human patients in clinical trials [11]. Cortical implants, such as the Monash Vision Group's Gennaris device[3], are still in the preclinical phase. However, cortical implants may be able to treat additional causes of blindness as the cortex is further *downstream* along the visual pathway. The cortex also has a larger surface area than the retina, which may allow vision with higher spatial resolution.

For a survey of IVP research and development, including many concepts in this paper, please refer to the extensive book edited by Dagnelie [8].

2 Limitations of Implanted Visual Prostheses

At a fundamental level, implanted visual prostheses operate by converting imagery from a headworn camera into spatial-temporal patterns of electrical stimulation applied to a patient's visual pathway. This is true for both cortical and retinal prostheses. The conversion process is usually performed on portable computational hardware, which is externally worn by the patient.

[2] http://www.eye-tuebingen.de/zrenner/retimplantlist/
[3] http://www.monash.edu.au/bioniceye/resources.html (Annual report 2013)

Figure 1 is a system overview of Monash Vision Group's cortical visual prosthesis [17], which contains stereotypical sub-systems shared by many other prostheses. Images are captured by a headworn camera and sent to a portable computer, the *Pocket Processor*. In real time, the pocket processor converts camera images into spatial-temporal patterns of electrical stimulation, which are conveyed over a wireless link. The implanted electrodes receives electrical power and signal from the wireless coil, which it uses to apply electrical stimulation to the visual cortex. A conceptual walkthrough of how the MVG device operates is available online: http://youtu.be/v9Ip8j3eca8.

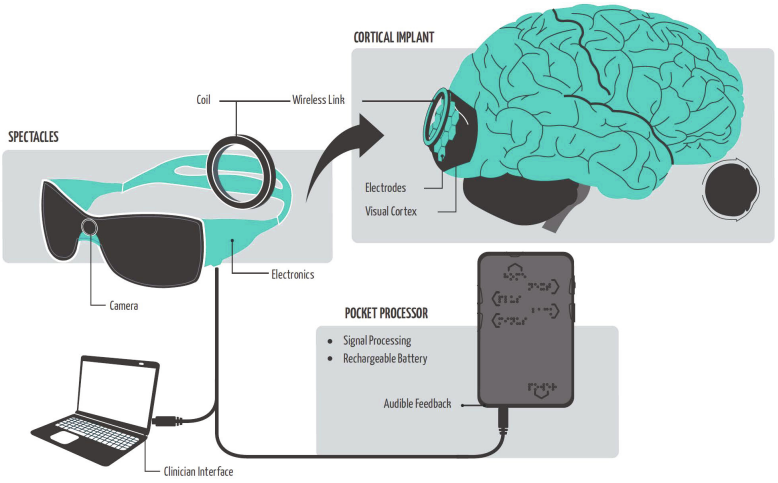

Fig. 1. Overview of the Monash Vision Group (MVG) Cortical Visual Prosthesis

2.1 Limited Spatial and Intensity Resolutions

The conversion from headworn sensor imagery to electrical stimuli is an ongoing research problem. While state-of-the-art stimulation regimes are able to reliably elicit phosphenes (bright visual percepts), the elicited phosphenes have poor dynamic range and can only be packed at low spatial resolutions. Figure 2 illustrates this using Simulated Prosthetic Vision (SPV), a technique pioneered in the early 1990's to simulate what an implanted patient may *see* [4]. The input image is converted into prosthetic vision using an adaptive thresholding approach [22] where a corresponding phosphene is enabled for bright regions of the input image. The SPV assumes the ability to generate 625 binary phosphenes, which is similar to the expected capabilities of the Monash Vision Group prosthesis [16].

The SPV image in Figure 2b clearly illustrates the severe information loss due to the limited spatial and intensity resolution of prosthetic vision. As the number of phosphenes generally corresponds to the number of implanted electrodes[4], the spatial resolution of prosthetic vision is limited by the factors such as the spread

[4] Coordinated activation of many electrodes may increase future phosphenes counts.

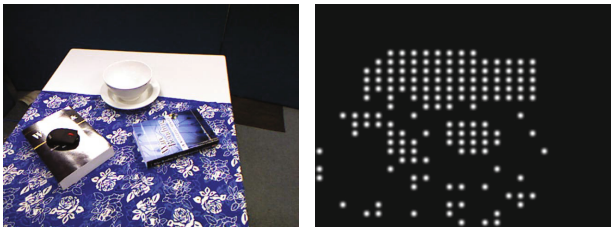

(a) Input (b) SPV

Fig. 2. Simulated Prosthetic Vision (SPV) from an implanted visual prostheses

of electrical charge, surgical safety of implantation and electrode fabrication technology. Improvement in these areas are slow as they often require lengthy preclinical and clinical trials.

Clinical studies of retinal prostheses [10] suggest that multiple levels of phosphene brightness can be achieved but *brightness ratings are likely to vary substantially across sessions and across subjects*. There is also evidence that phosphenes of multiple levels of intensity can be produced by varying stimulation currents [20], but changes in phosphene brightness may be coupled with changes in phosphene shape and size. There is little evidence that phosphene brightness can be varied consistently with a cortical prosthesis. As such, the work presented below assumes the *worst case* of binary phosphenes.

Arguably, Dobelle was the first to consider the use of computer vision to improve the usefulness of prosthetic vision [9]. More recently, simple IVP computer vision algorithms were developed to run on wearable devices with embedded processors [23,29]. More sophisticated IVP vision algorithms have also been investigated using less portable computers. *Transformative Reality* [18] uses multiple sensing modalities to better *render* a pattern of phosphenes representing models of the world. The substantial body of work on *Vision Processing for prosthetic vision* [1] applies computer vision algorithms to improve simulated multi-intensity phosphene patterns for reading text, navigation and other tasks.

2.2 Irregular Phosphene Maps

A patient's *Phosphene Map* contains all the phosphenes that can be elicited by electrical stimulation. Older IVP research, including work on image processing and computer vision, generally assumes regular phosphene maps similar to the map shown in Figure 3a. However, there is strong clinical and biological evidence to suggest that phosphene maps are irregular and patient-specific [3,19,27]. An example of an irregular phosphene map is shown in Figure 3b.

Apart from irregular locations and sizes, there is also evidence that phosphenes can exhibit irregular *shapes*. Studies from Bionic Vision Australia[5] and Second Sight [19] show that the shape of phosphenes can be anisotropic and the shape of phosphenes may vary depending on electrical stimulation.

[5] http://goo.gl/LwcGwO

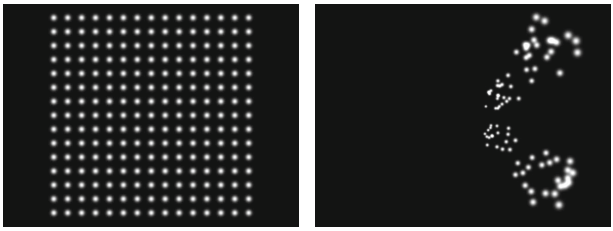

(a) Regular (b) Irregular

Fig. 3. Example of Regular and Irregular phosphene maps

The computer vision system presented in this paper has the potential to accommodate all three aspects of phosphene map irregularity: location, size and shape. However, as the MVG device is still in the preclinical stage, the system is only tested on phosphene maps simulated based on electrical, surgical and cortical models. These models only generate irregularities in phosphene locations and sizes. The simulation assumes that phosphenes appear as isotropic Gaussians as recommended by the survey of simulated prosthetic vision by Chen *et al* [5]. Details of the simulation are available in Section 3.1.

3 Computer Vision System for IVP

Despite the reality that Implanted Visual Prostheses (IVP) produce irregular phosphene maps, very little research has been done to address the problem in full. Research that attempts to deal with irregular phosphene maps generally only do so for *near-regular* mappings where small spatial shifts in phosphene locations and electrode dropouts are modelled [25] or only irregular phosphene shapes are considered over a regular grid [14].

More importantly, many systems do not run in real time on an embedded processor suitable for a wearable medical device. Clinical trials of retinal implants [28] and cortical implants [21] suggest that prosthetic vision may have refresh rates as high as 10Hz. Simulated Prosthetic Vision trials show that low refresh rates may reduce task performance [13]. Therefore, a practical IVP requires a fast and flexible computer vision system.

Given the background above, this paper provides the following contributions:

1. Section 3.1 describes a detailed simulation of a cortical IVP device
2. Section 3.2 details a computer vision system that deals with irregular phosphene maps using a second mapping called the Camera Map to provide flexibility.
3. Section 3.3 details a fast image processing method for the vision system.
4. Section 3.4 details a simulated prosthetic vision visualisation that shows the phosphenes *seen* by a patient in real time.
5. Section 3.5 summarises the real time performance of the system.

3.1 Simulating a Cortical Implanted Visual Prosthesis

Phosphene maps were simulated in order to test the computer vision system. The simulation is based on the Monash Vision Group (MVG) cortical Implanted Visual Prothesis (IVP), which is currently undergoing preclinical trials. Parameters of the MVG IVP system were obtained from published sources [16,17].

The main components of the simulation are detailed on the left of Figure 4 (in red). The simulation starts with the definition of the spatial layout of an implanted electrode array. The array is also known as a *tile*. The MVG IVP uses multiple identical tiles. A tile contains 43 active electrodes. The MVG *Tile Layout* is shown at the top left of Figure 4 with blue dots representing electrodes.

Next, the simulation places multiple tiles onto the surface of the visual cortex. Coordinates on the visual cortex are defined on a *Cortical Plane*, which represents a flattened cortical surface. *Tile Locations* are defined using 2D affine transforms. This results in a list of *Ideal Electrode Locations* on the cortical plane. A surgical scenario proposed by a MVG Neurosurgeon is shown at the middle-left of Figure 4. The four-tile wedge-shaped arrangement avoids the Calcarine Sulcus, which is a large crevice on the visual cortex.

The simulation then applies two sources of irregularities that simulate real world issues: Electrode dropouts and the imprecise placement of electrodes. The *Dropout Rate* models implanted electrodes that fail to elicit a phosphene when stimulated electrically. For example, a dropout rate of 50% means that half of all implanted electrodes cannot be used to elicit a phosphene. Electrode dropouts have been reported in multiple IVP clinical trials [11,32], but generally at rates lower than 50%.

Spatial Error models several issues by approximating their combined effect as a normally distributed 2D random offset defined on the cortical plane. For example, electrode deformation during surgical insertion and variations in cortical anatomy are both factors that can be approximated as spatial error. The application of dropouts and spatial error results in *Irregular Electrode Locations*, an example of which can be seen at the bottom-left of Figure 4.

Finally, a *Cortical Model* is applied to estimate the locations of phosphenes in the visual field. The cortical model, also known as a visuotopic map or retinotopy, relates spatial regions on the cortical plane to corresponding regions in the visual field. For the MVG IVP, the cortical model exhibits a *log-polar* relationship, where regions in central vision are mapped to larger cortical regions than regions in peripheral vision. This phenomenon is known as *cortical magnification*. Detailed illustrations of cortical models showing magnification and retinotopy can be found in [26].

As the MVG IVP uses multiple electrode tiles implanted near the occipital lobe, the electrodes will electrically stimulate regions of the primary visual cortex (V1) primarily corresponding to central vision. As such, the simulation uses the Monopole cortical model [24]:

$$z = \exp(\frac{w}{k}) - a \qquad (1) \qquad\qquad m = \frac{E + a}{k} \qquad (2)$$

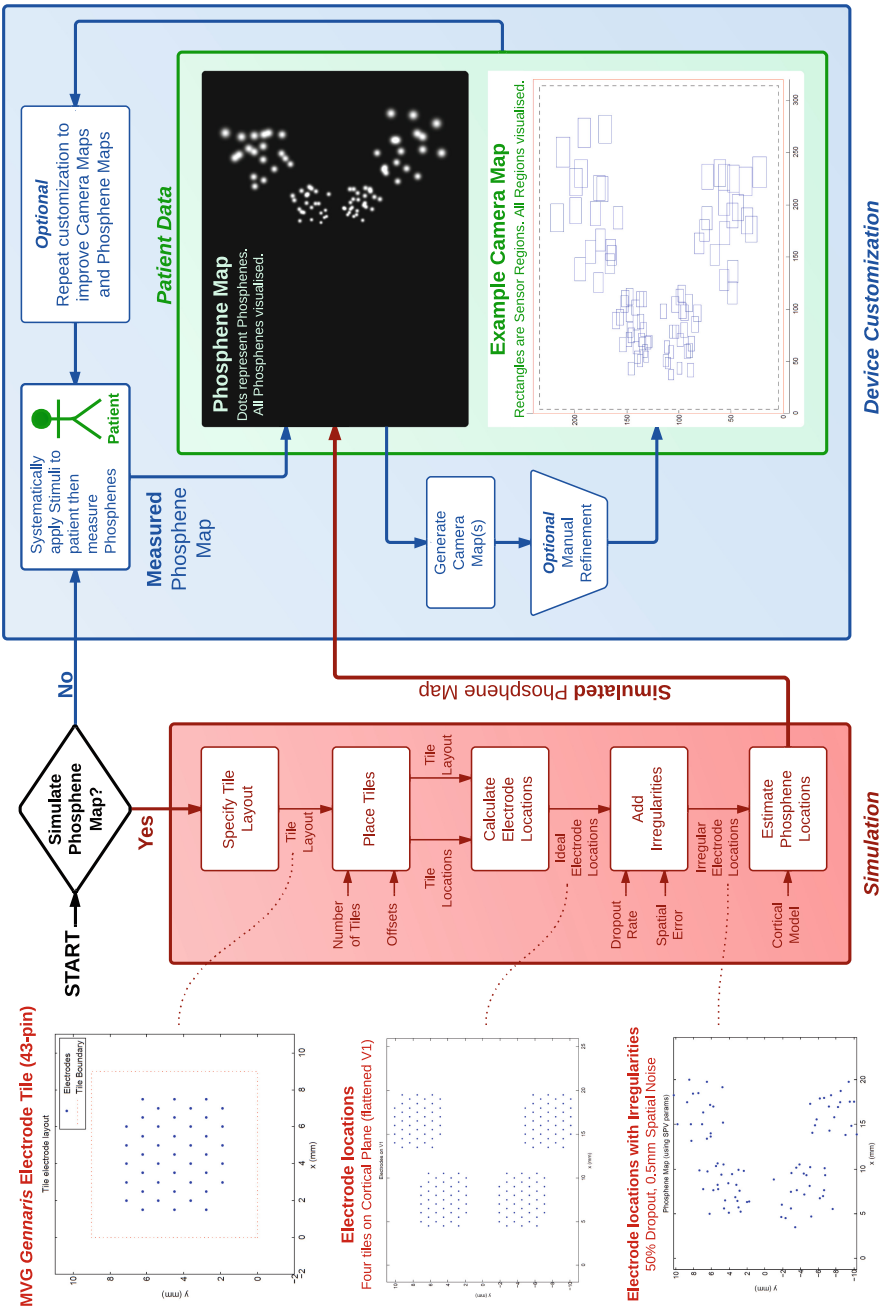

Fig. 4. System for the Simulation and Generation of Patient Data

The variable w is a complex variable representing the 2D spatial location of an electrode on the cortical plane as $w = x + iy$. z is a complex variable representing the corresponding spatial location of phosphenes in the visual field. E is the Eccentricity, which is an angle radiating from the center of the visual field. m is the cortical magnification, which increases the size of phosphenes further from the center of the visual field. k and a are constants that model the cortical magnification and the location of central vision. The values of $k = 15$ and $a = 0.7$ were selected based on typical values used in human models.

Figure 5 contains Simulated Prosthetic Vision (SPV) visualisations of simulated phosphene maps generated assuming four MVG tiles implanted on the left primary visual cortex (See middle-left of Figure 4). The locations and sizes of phosphenes in the visual field are governed by Equations 1 and 2. The SPV visualisation covers around 10 degrees of the visual field. The phosphenes are on the right visual hemisphere as the left visual cortex is being stimulated.

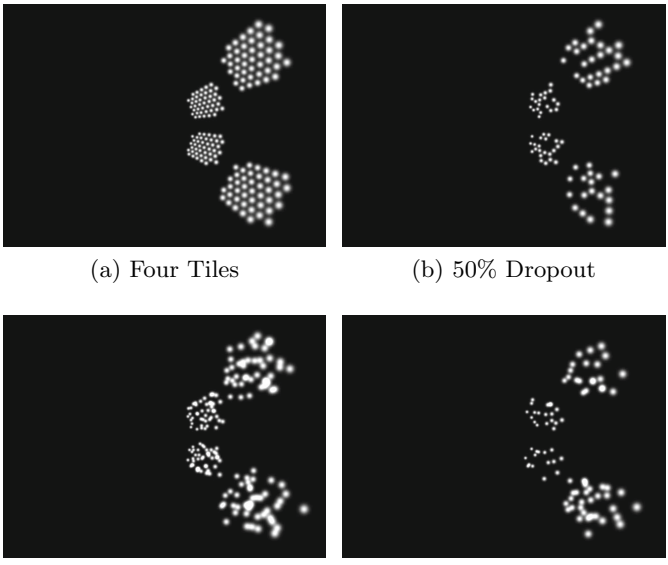

(a) Four Tiles (b) 50% Dropout

(c) Spatial Error $\sigma = 0.5$mm (d) Spatial & Dropout

Fig. 5. SPV visualisations of phosphene maps for the MVG IVP

3.2 Dealing with Irregular Phosphene Maps Using Camera Maps

A key innovation of the proposed IVP computer vision system is the use of **two** mappings: A Phosphene Map and a Camera Map.

Phosphene Map
A mapping between **Stimuli** and **Phosphene**.

Camera Map
A mapping between **Stimuli** and **Regions in the Camera Image**.

Stimuli is defined as electrical stimulation that elicits phosphenes. For the sake of simplicity, the work in this paper assumes that a single electrode can trigger a stimulus which in turn produces only one phosphene. In other words, it is assumed that one working electrode can produce one phosphene. This assumption is the norm in current IVP research. For reasons detailed in Section 2.1, only binary phosphenes are considered. Note however that the proposed system can be extended to deal with more complex assumptions, such as multi-level phosphenes or many-to-many mappings between stimuli and phosphenes.

An irregular phosphene map is visualised on the middle-right of Figure 4. In practice, a phosphene map is either obtained by simulation or psychophysics measurements performed on the implanted patient. The latter is commonly referred to as *Phosphene Mapping*, which involves the adjustment of electrical stimulation while obtaining patient feedback regarding phosphene appearance. Phosphene mapping dates back to the pioneering work of Brindley and Lewin [2]. A patient's phosphene map is expected to be nearly constant over time, but factors such as electrode dropouts may lead to small changes.

Existing IVP computer vision systems usually assume near-regular phosphene maps and also uses the phosphene map as the spatial layout for image processing. For example, Figure 2 shows a down sampling operation carried out using a spatial layout based on a regular phosphene map. Irregular phosphene maps have also been used to directly specify image processing regions [30].

However, the phosphene map is a measurement that approximates the *true* phosphenes experienced by the patient during stimulation by implanted electrodes. It basically represents the state of the patient-electrode interface. To modify how image processing is performed spatially, existing systems have to modify the phosphene map. This *one-map* approach confuses the *inflexible* phosphene map with the relatively flexible and arbitrary spatial mappings that can be used for image processing operations.

Unlike existing approaches, the proposed IVP computer vision system does not use the phosphene map to perform image processing operations. Instead, the phosphene map is only used by the system to perform real time visualisations, as detailed in Section 3.4. Image processing is performed using a *Camera Map*, which contains a set of mappings between stimuli and regions in the camera image. Figure 6 explains the relationship between a camera map and phosphene map. Essentially, the stimuli relates both maps by acting as an index into the phosphene map and the camera map.

The motivation of having two separate maps is to decouple the state of the patient-electrode interface from how image processing is performed. The system treats the phosphene map as a constant mapping measured by clinicians while the camera map can be continually redesigned by engineers. The camera map can also be modified according to patient preferences and clinician recommendations.

The bottom right of Figure 4 shows a camera map generated from the phosphene map above it. Each rectangle represents a camera image region that is processed to determine whether to activate the corresponding phosphene. Regions in the camera map can be manually moved, scaled, reshaped and even

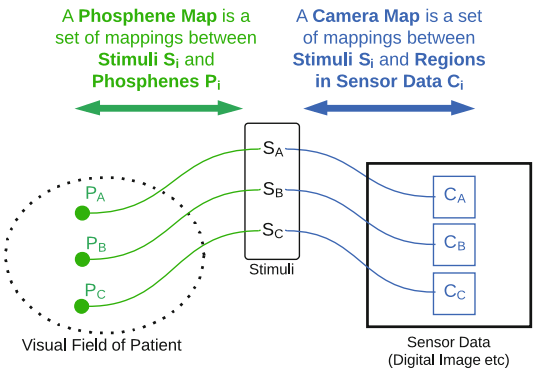

Fig. 6. Relationship between Phosphene Map and Camera Map

removed if needed; the latter can be used to disable a camera region in response to electrode dropouts. Also note that while this paper only considers rectangular regions, this two-map approach can be extended to irregularly shaped regions.

Another benefit of using a two-map approach is that while there is only one *true* phosphene map for an individual patient, there can be many possible corresponding camera maps. Figure 7 shows 3 camera maps for a two-tile phosphene map. The *Standard* camera map has image regions based on the size and location of corresponding phosphenes. The *Zoomed* camera map only covers the center of the camera image, which acts as a zoom function. The smaller regions may also be useful for the patient when viewing finer detail while panning the camera over a scene. Finally, the *Large* camera map shows the use of overlapping regions that mimic retinal receptive fields when processed using a Laplacian filter.

Image processing is performed with a camera map according to the process in Figure 8. Each region C_i in the camera map is processed independently. The results of the processing is used to decide whether to activate the corresponding phosphene P_i. For example, a system that shows bright objects can be built using a binary thresholding operation, where a phosphene is activated when the corresponding region has a mean intensity above a threshold value.

3.3 Fast Image Processing Using Integral Images

This section describes a fast thresholding method that quickly processes regions of a camera map. The method was implemented using C++ and platform-specific SIMD intrinsics for the MVG Wearable Prototype (Pocket Processor) shown in Figure 10. The thresholding method is described by Algorithm 3.1.

The inputs of the method are a gray sub-image (Region-of-Interest from headworn camera image), threshold value ("thVal"), threshold mode ("thMode") and a Stimuli Buffer where each element represents a Stimuli S_i corresponding to camera map region C_i (see Figure 6). The threshold mode can be *Manual*, where a threshold value is chosen by the patient via key presses, or *Auto*, where Otsu's method [22] is used to find a threshold automatically. The method outputs a

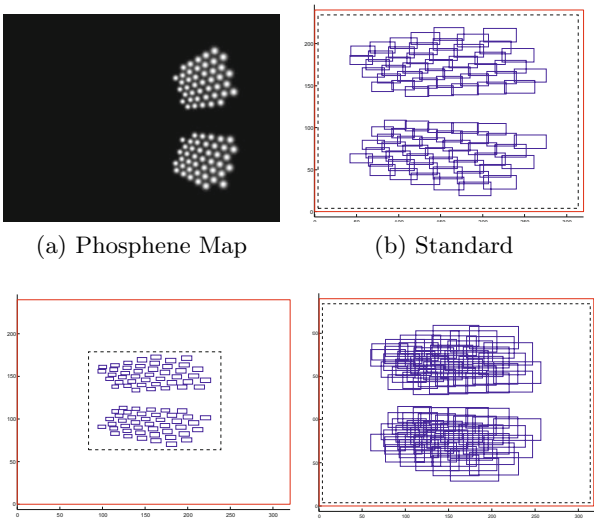

(a) Phosphene Map (b) Standard

(c) Zoomed (d) Large

Fig. 7. Several Camera Maps for a Two-Tile Phosphene Map

stimuli buffer where a *high* value in element S_i will produce electrical stimulation that elicits the corresponding phosphene P_i. It also outputs the threshold value ("thValUsed") when operating in automatic threshold mode.

The *integral*() function computes an integral image. Integral Images came from the Summed Area Table concept in Computer Graphics, which was first described by Crow [7]. The concept was later popularized by the work of Viola and Jones [31], who used integral images to rapidly compute the sum of pixel regions to calculate Haar-like features. The $fastmean()$ function in the algorithm uses integral images to quickly calculate the mean of a region ($sum/count$).

Note that the integral image only has to be calculated once for an input image in order to allow fast mean computation for practically any number of rectangular regions. As the majority of computational time rests with the *integral*() function instead of the $fastMean()$ function, the method has a predictable running time that is independent of the camera map. This is true even for Camera Maps with many overlapping regions such as the one shown in Figure 7d.

The *threshold*() function in Algorithm 3.1 takes "thSrc" as input and outputs into "thDst", both of which are small arrays with size equal to the number of enabled regions in the camera map. Regions in the camera map can be disabled in response to electrode dropouts, patient or clinician requests or algorithm-specific reasons. Elements in "thDst" are set to *high* if the corresponding element in "thSrc" is above the threshold value. Otherwise the element is set to zero.

The method described above operates within the pocket processor sub-system of the MVG device in Figure 1. The pocket processor also generates audio cues, accepts user inputs, provides a clinician interface for the modification of

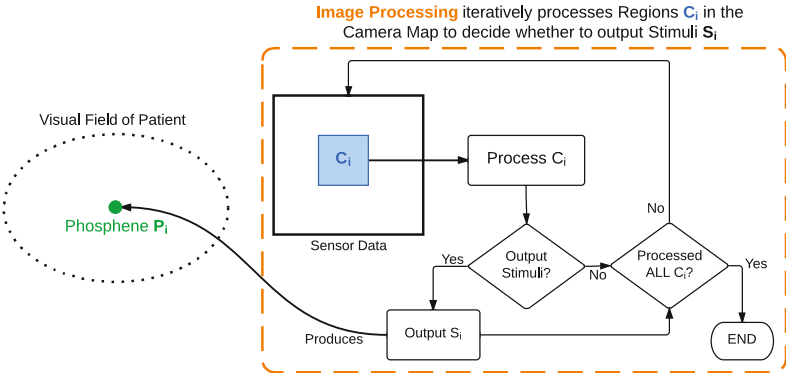

Fig. 8. Image processing using a Camera Map

Algorithm 3.1 Fast Threshold using Integral Images

Input: $grayImage$, $thVal$, $thMode$, $stimuliBuffer$
Output: $stimuliBuffer \leftarrow array(int)$, $thValUsed$

```
stimuliBuffer ← 0, e ← 0
integralImage ← integral(grayImage)
for all i ← {0, rect.length() − 1} do
    if enable[i] then
        thSrc[e] ← fastMean(integralImage, rect[i])
        e ← e + 1
thValUsed ← threshold(thSrc, thDst, thVal, thMode)
j ← 0
for all i ← {0, numEnabled − 1} do
    if enable[i] then
        stimuliBuffer[i] ← thDst[j]
        j ← j + 1
```

stimulation parameters and outputs stimulation commands to the wireless system. Details of these additional functionalities are outside the scope of this paper.

3.4 Real Time SPV Visualisation Using Phosphene Map

A fast Simulated Prosthetic Vision (SPV) visualisation algorithm was also implemented in C++ for the MVG pocket processor. It uses the patient's phosphene map and the stimuli buffer output of the fast image processing method to render a 640×480 image of activated phosphenes. This provides a real time visualisation of the prosthetic vision experienced by a patient, which is useful for engineers making adjustments to image processing parameters and for clinicians modifying stimulation parameters or guiding patients through psychophysics activities. The visualisation is disabled during daily use to reduce computational and power costs as the vision impaired patient do not need this functionality.

SPV visualisations captured during system testing are shown in Figures 9a and 9b. The left side of the visualisation contains the camera image overlaid with regions defined in the camera map. The results of image processing, the activated phosphenes, are shown on the right. The phosphene map is the same as the four-tile map in Figure 5a.

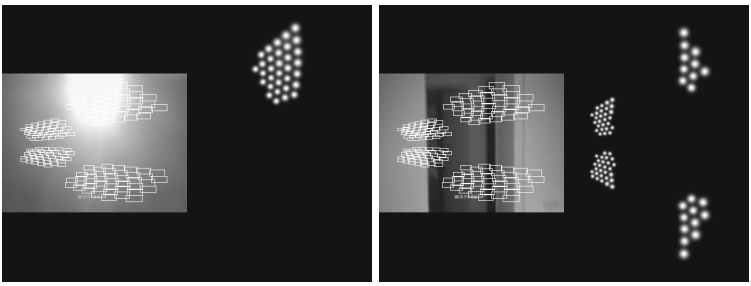

(a) Images from wearable camera

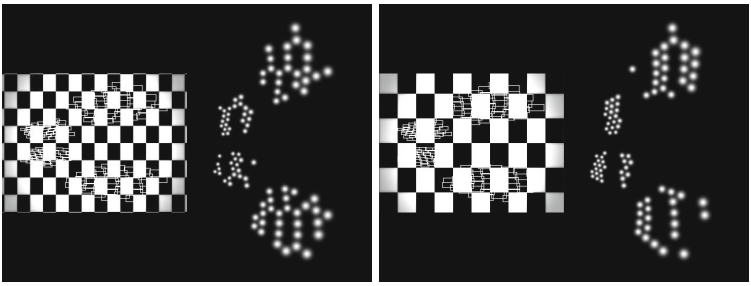

(b) Offline testing with synthetic images

Fig. 9. Real Time SPV visualisations

Phosphenes are drawn using template images that are pre-generated by the simulation described in Section 3.1. A pixel texture is copied to a region of interest in the SPV visualisation image in a similar way as the *blit* operation available in many graphics libraries.

3.5 System Testing and Results

The computer vision system was tested on the MVG wearable prototype in Figure 10. As the MVG device is still in the preclinical phase, system testing was performed using the simulated phosphene map from Figure 5a. The camera map used for testing can be seen in the SPV visualisations in Figures 9. Real time system operation and SPV visualisations for different mappings can be seen in the videos accompanying the paper[6].

[6] http://goo.gl/fBKpWT

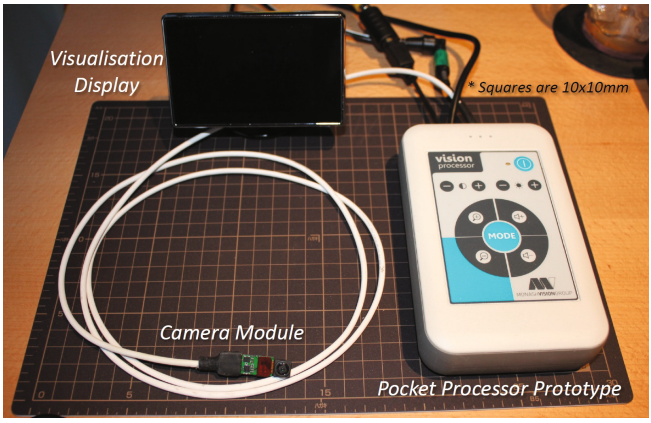

Fig. 10. Wearable Hardware Prototype for Software Development and Testing

Processing times measured over 400 images from the camera module (640×480):

	Mean (ms)	**STD (ms)**	**Min (ms)**	**Max (ms)**
Image Processing	2.53	0.14	2.41	2.69
SPV Visualisation	1.98	0.37	1.03	2.87

4 Discussion and Conclusions

This paper presented a real time computer vision system for implanted visual prostheses. The system uses a novel second mapping called the Camera Map, decoupling the invariant patient-electrode interface from the highly flexible pixel regions used for image processing. The system is fast, taking only several milliseconds to perform image processing and visualisation.

Future work will focus on two aspects. Firstly, the computer vision system will be integrated into ongoing psychophysics trials measuring task performance [12] and evaluating thresholding approaches [6]. Secondly, additional image processing modes will be implemented for the computer vision system.

Acknowledgements. Monash Vision Group is funded through the Australian Research Council Research in Bionic Vision Science and Technology Initiative (SR1000006). The author thanks the anonymous reviewers for their insightful comments.

References

1. Barnes, N.: An overview of vision processing in implantable prosthetic vision. In: IEEE International Conference on Image Processing, pp. 1532–1535, September 2013
2. Brindley, G.S., Lewin, W.S.: The sensations produced by electrical stimulation of the visual cortex. The Journal of Physiology **196**, 479–493 (1968)

3. Buffoni, L.X., Coulombe, J., Sawan, M.: Image processing strategies dedicated to visual cortical stimulators: a survey. Artificial Organs 29(8), 658–64 (2005). http://www.ncbi.nlm.nih.gov/pubmed/16048483
4. Cha, K., Horch, K., Normann, R.A.: Simulation of a phosphene-based visual field: visual acuity in a pixelized vision system. Annals of Biomedical Engineering **20**(4), 439–449 (1992)
5. Chen, S.C., Suaning, G.J., Morley, J.W., Lovell, N.H.: Simulating prosthetic vision: I. Visual models of phosphenes. Vision Research **49**(12), 1493–1506 (2009)
6. Collette, M., Horace, J., Lindsay, K., Wai Ho, L.: The Impact of Luminance Threshold Modes and Phosphene Dropout Rates in Psychophysics Testing for the Monash Vision Group's Cortical Vision Prosthesis Gennaris. Frontiers in Human Neuroscience 7 (2013)
7. Crow, F.: Summed-area tables for texture mapping. In: ACM SIGGRAPH Computer Graphics. 18, pp. 207–212, July 1984. http://dl.acm.org/citation.cfm?id=808600
8. Dagnelie, G.: Visual Prosthetics. Springer, US, Boston, MA (2011)
9. Dobelle, W.H.: Artificial vision for the blind by connecting a television camera to the visual cortex. ASAIO Journal (American Society for Artificial Internal Organs: 1992) 46(1), 3–9 (2000). http://www.ncbi.nlm.nih.gov/pubmed/10667705
10. Greenwald, S.H., Horsager, A., Humayun, M.S., Greenberg, R.J., McMahon, M.J., Fine, I.: Brightness as a function of current amplitude in human retinal electrical stimulation. Investigative Ophthalmology & Visual Science **50**(11), 5017–5025 (2009)
11. Humayun, M.S., Dorn, J.D., da Cruz, L., Dagnelie, G., Sahel, J.A., Stanga, P.E., Cideciyan, A.V., Duncan, J.L., Eliott, D., Filley, E., Ho, A.C., Santos, A., Safran, A.B., Arditi, A., Del Priore, L.V., Greenberg, R.J.: Interim results from the international trial of Second Sight's visual prosthesis. Ophthalmology **119**(4), 779–788 (2012)
12. Josh, H., Mann, C., Kleeman, L., Lui, W.L.D.: Psychophysics testing of bionic vision image processing algorithms using an FPGA Hatpack. In: 2013 IEEE International Conference on Image Processing, pp. 1550–1554. IEEE, September 2013, http://ieeexplore.ieee.org/lpdocs/epic03/wrapper.htm?arnumber=6738319
13. Josh, H., Yong, B., Kleeman, L.: A Real-time FPGA-based Vision System for a Bionic Eye. In: ARAA (ed.) Proceedings of Australasian Conference on Robotics and Automation. p. Online. ARAA, Melbourne, Australia (2011)
14. Kiral-Kornek, F.I., Savage, C.O., O'Sullivan-Greene, E., Burkitt, A.N., Grayden, D.B.: Embracing the irregular: A patient-specific image processing strategy for visual prostheses. In: International Conference of the IEEE Engineering in Medicine and Biology Society 2013, 3563–3566, January 2013. http://www.ncbi.nlm.nih.gov/pubmed/24110499
15. LeRoy, C.: Ou l'on rend compte de quelques tentatives que l'on a faites pour guerir plusieurs maladies par l'electricite. In: (Paris), H.A.R.S. (ed.) Memoires Math. Phys., pp. 87–89 (1755)
16. Li, W.H.: Wearable Computer Vision Systems for a Cortical Visual Prosthesis. In: 2013 IEEE International Conference on Computer Vision Workshops, pp. 428–435. IEEE, December 2013
17. Lowery, A.J.: Introducing the Monash vision group's cortical prosthesis. In: 2013 IEEE International Conference on Image Processing, pp. 1536–1539. IEEE, September 2013

18. Lui, W.L.D., Browne, D., Kleeman, L., Drummond, T., Li, W.H.: Transformative reality: Augmented reality for visual prostheses. In: 2011 10th IEEE International Symposium on Mixed and Augmented Reality, pp. 253–254. IEEE, October 2011. http://doi.ieeecomputersociety.org/10.1109/ISMAR.2011.6092402http://youtu.be/J30uYYkDApYhttp://youtu.be/iK5ddJqNuxY
19. Nanduri, D., Humayun, M.S., Greenberg, R.J., McMahon, M.J., Weiland, J.D.: Retinal prosthesis phosphene shape analysis. In: International Conference of the IEEE Engineering in Medicine and Biology Society 2008, pp. 1785–1788, January 2008. http://www.ncbi.nlm.nih.gov/pubmed/19163027
20. Nanduri, D., Humayun, M.S., Weiland, J.D., Dorn, J., Greenberg, R.J., Fine, I.: Encoding of size and brightness of percepts in a visual prosthesis, September 2013. http://www.google.com/patents/US8527056
21. Naumann, J.: Search for Paradise: A Patient's Account of the Artificial Vision Experiment. Xlibris (2012). http://www.amazon.com/Search-Paradise-Artificial-Experiment-ebook/dp/B009A86X9K
22. Otsu, N.: A Threshold Selection Method from Gray-Level Histograms. Ieee Transactions On Systems Man And Cybernetics **9**, 62–66 (1979)
23. Parikh, N., Itti, L., Weiland, J.: Saliency-based image processing for retinal prostheses. Journal of neural engineering 7(1), 16006 (2010). http://www.ncbi.nlm.nih.gov/pubmed/20075505
24. Polimeni, J.R., Balasubramanian, M., Schwartz, E.L.: Multi-area visuotopic map complexes in macaque striate and extra-striate cortex. Vision Research **46**(20), 3336–3359 (2006)
25. van Rheede, J.J., Kennard, C., Hicks, S.L.: Simulating prosthetic vision: Optimizing the information content of a limited visual display. Journal of Vision **10**(14), 1–14 (2010)
26. Schiller, P., Tehovnik, E.: Visual Prosthesis. Perception **37**, 1529–1559 (2008)
27. Srivastava, N.R.: Simulations of Cortical Prosthetic Vision. In: Dagnelie, G. (ed.) Visual Prosthetics, pp. 355–365. Springer (2011)
28. Stingl, K.K.T., Bartz-Schmidt, K.U., Besch, D., Braun, A., Bruckmann, A., Gekeler, F., Greppmaier, U., Hipp, S., Hörtdörfer, G., Kernstock, C., Koitschev, A., Kusnyerik, A., Sachs, H., Schatz, A., Peters, T., Wilhelm, B., Zrenner, E.: Artificial vision with wirelessly powered subretinal electronic implant alpha-IMS. Proceedings. Biological sciences / The Royal Society 280(1757), 20130077 (2013). http://rspb.royalsocietypublishing.org/content/280/1757/20130077.abstract
29. Tsai, D., Morley, J.W., Suaning, G.J., Lovell, N.H.: A wearable real-time image processor for a vision prosthesis. Computer methods and programs in biomedicine 95(3), 258–69 (2009). http://www.ncbi.nlm.nih.gov/pubmed/19394713
30. Veraart, C., Wanet-Defalque, M.C., Gerard, B., Vanlierde, A., Delbeke, J.: Pattern Recognition with the Optic Nerve Visual Prosthesis. Artificial Organs **27**(11), 996–1004 (2003)
31. Viola, P., Jones, M.: Rapid object detection using a boosted cascade of simple features. In: Proceedings of the 2001 IEEE Computer Society Conference on Computer Vision and Pattern Recognition, CVPR 2001, pp. 511–518. IEEE (2001). http://ieeexplore.ieee.org/lpdocs/epic03/wrapper.htm?arnumber=990517
32. Wilke, R., Gabel, V.P., Sachs, H., Bartz Schmidt, K.U., Gekeler, F., Besch, D., Szurman, P., Stett, A., Wilhelm, B., Peters, T., Harscher, A., Greppmaier, U., Kibbel, S., Benav, H., Bruckmann, A., Stingl, K., Kusnyerik, A., Zrenner, E.: Spatial resolution and perception of patterns mediated by a subretinal 16-electrode array in patients blinded by hereditary retinal dystrophies. Investigative Ophthalmology & Visual Science **52**(8), 5995–6003 (2011)